Volume 17
Number 2
Dec 2025

Journal of
The Indonesian Society of Integrated Chemistry
Published by Jambi University, Chemistry Education Study Program

P-ISSN 2085-1715 & E-ISSN 2621-5543

JISIC

Kinetics and Adsorption Efficiency of Fe(III) by Fe-IIP Adsorbent for Water Remediation

Felisa Nadia Oktavira Putri Surya[1], Maria Monica Sianita Basukiwardojo[2*],

[1,2]Kimia, Universitas Negeri Surabaya

ABSTRACT

Iron (Fe) is an essential metal that plays a vital role in various biological and environmental processes. However, excessive concentrations of Fe, particularly in the form of Fe(III), can cause toxic effects, disrupt aquatic ecosystems, and pose serious risks to human health. This study aims to develop a selective adsorbent based on an Fe(III)-imprinted polymer (Fe(III)-IIP) for removing Fe(III) contamination from water. The Fe(III)-IIP was synthesized through precipitation polymerization using $Fe(NO_3)_3$, EDTA, MAA, EGDMA, and BPO as the main components. FTIR spectroscopy confirmed the presence of Fe–O functional groups and the successful removal of template ions. SEM analysis revealed a porous surface morphology with a uniform particle distribution, supporting enhanced adsorption capacity. Adsorption experiments were performed at contact times ranging from 30 to 180 minutes to determine the optimum condition. The results showed that adsorption efficiency increased with contact time, reaching equilibrium at 30 minutes with an adsorption capacity of 4.43 mg g^{-1}, consistent with a pseudo-second-order (PSO) kinetic model. These findings demonstrate that Fe(III)-IIP is an effective adsorbent for treating Fe(III)-contaminated water.

Keywords: Adsorption, Fe(III), IIP, Contact time

Received: November, 13 2025;
Revised: November, 25 2025;
Accepted: December, 15 2025

* Corresponding author: mariamonica@unesa.ac.id
DOI: https://doi.org/10.22437/jisic.v17i2.49878

INTRODUCTION

Iron (Fe) is an essential metal that plays a vital role in various physiological and environmental processes. It participates in oxygen transport, enzyme activation, and numerous biochemical reactions, and is abundantly distributed in the Earth's crust. In aquatic and environmental systems, iron primarily exists in two oxidation states: Fe(II) and Fe(III) (Zhang *et al*., 2024). Under oxygen-rich conditions, Fe(II) is unstable and easily oxidized to insoluble Fe(III) hydroxides. While iron is necessary in trace amounts, excessive Fe(III) can be harmful to both humans and the environment (Sappewali *et al*., 2024).

High concentrations of Fe(III) in water can alter its appearance and chemical properties, making it turbid, acidic, and unsuitable for consumption. It may also form deposits that damage aquatic habitats.

In humans, prolonged exposure to high levels of iron can cause serious health problems, including organ damage, nervous system disorders, and other complications (Rahma *et al*., 2023). Therefore, removing excess Fe(III) from polluted water is an important step in environmental protection and public health.

Several conventional methods have been employed to remove iron from water, including coagulation (Sufra *et al*., 2024), ion exchange (Putri *et al*., 2023), membrane filtration (Veranica *et al*., 2023), and various chemical treatments. However, these methods still face several challenges, including low selectivity, high operating costs, and the generation of secondary waste. Consequently, there is growing interest in developing more efficient and environmentally friendly materials for Fe(III) removal.

One promising approach is the use of polymer-based adsorbents, which are stable, reusable, and maintain their structural integrity. Among these, ion-imprinted polymers (IIPs) have attracted attention for their high selectivity toward target ions. The imprinting process creates specific binding sites in the polymer matrix that match the size, shape, and coordination environment of the target ion (Ngatijo *et al*., 2019). Despite the presence of other ions, IIPs are effective in selectively and strongly adsorbing the desired ions. The stability of IIPs depends on the adsorption process, making them suitable for multiple reuse cycles (Low *et al*., 2024). These features make IIPs an excellent choice for removing Fe(III) from water.

Many studies have demonstrated the successful synthesis and application of Fe(III)-imprinted polymers. However, further research is needed to improve their performance and understand the factors that affect adsorption behavior. For instance, the contact time between the polymer and Fe(III) ions significantly influences how well the active sites can bind to the target ions (Royani *et al*., 2024). Djunaidi *et al*. (2021) reported that poly(eugenol)-based IIPs with PEGDE as a crosslinker achieved an adsorption capacity of 23.64 mg/g after 60 minutes, following a pseudo-second-order kinetic model. Meanwhile, Royani *et al*. (2024) found that Fe(III)-imprinted polymers synthesized via a cooling–heating method reached equilibrium after 40 minutes, showing an adsorption capacity of 9.35 mg/g, which followed the pseudo-first-order model. These studies suggest that both the synthesis method and polymer matrix composition strongly influence the adsorption kinetics and overall performance of IIP materials.

Despite progress in IIP research, the kinetics and adsorption efficiency on Fe(III) adsorption using precipitation polymerization have not been extensively explored. The adsorption efficiency of IIPs depends on how long Fe(III) ions interact with the polymer's active binding sites. Therefore, this study aims to synthesize Fe(III)-imprinted polymers (Fe(III)-IIP) using precipitation polymerization and evaluate their adsorption behavior over various contact times. The results are expected to provide new insights into adsorption kinetics and efficiency, helping identify the optimal conditions for Fe(III) removal and supporting the development of effective, reusable materials for water treatment.

METHODS

Tools and Materials

The materials used in this research were ferric nitrate ($Fe(NO_3)_3$, Merck), methacrylic acid (MAA, Sigma Aldrich), ethylene glycol dimethacrylate (EGDMA, Merck), ethylenediaminetetraacetic acid (EDTA, Merck), benzoyl peroxide (BPO, Merck), ethanol (Merck), acetonitrile (Merck), concentrated nitric acid (HNO_3, Merck), concentrated hydrochloric acid (HCl, Merck), distilled water (aquades), and double-distilled water (aquabides).

The tools used in this research were Atomic Absorption Spectroscopy (AAS, Shimadzu AA-7000), Fourier Transform Infrared Spectroscopy (FTIR, Perkin Elmer Spectrum One), and Scanning Electron Microscopy (SEM, ZEISS Evo 10). Additional laboratory equipment included spatulas, reagent bottles, beakers, 100 mL Erlenmeyer flasks, 100 mL volumetric flasks, test tubes, graduated pipettes, volumetric pipettes, dropper pipettes, thermometers, glass funnels, magnetic stirrers, petri dishes, and micropipettes. Filtration procedures were carried out using a standard laboratory filtration system.

Synthesis of Ionic Imprinted Polymer (IIP)

To initiate pre-polymerization complex formation, 0.1 mmol of Fe(NO3)3 was dissolved in 60 mL of an ethanol–acetonitrile mixture (2:1, v/v) along with 0.25 mmol of EDTA and stirred for 30 minutes. Subsequently, 4 mmol of MAA was added as the functional monomer, 20 mmol of EGDMA as the crosslinker, and 0.2 mmol of BPO as the initiator. Before polymerization, the mixture was degassed under nitrogen for 5 minutes to remove oxygen, then sealed with aluminum foil and polymerized at 70°C in a water bath under constant stirring. The resulting polymer was filtered, thoroughly washed with ethanol and aquabides, and then dried in an oven at 60°C until a constant weight.

Leaching of Ionic Imprinted Polymer (IIP)

The template ion was removed by leaching with 100 mL of 3 M HNO3 under continuous stirring for 3 hours. The leached polymer was repeatedly rinsed with distilled water until the pH reached neutrality, then filtered and dried in an oven at 60°C to obtain the Ion-Imprinted Polymer (IIP). The filtrate obtained from the leaching process was analyzed by atomic absorption spectroscopy (AAS) to determine the concentration of leached Fe(III) ions. The leaching efficiency was calculated using the following equation 1:

$$\text{Leaching (\%)} = \frac{Ci - Cf}{Ci} \times 100\% \qquad (1)$$

Where Ci (mg/L) is the initial concentration of the template ion, and Cf (mg/L) is the remaining concentration after leaching.

Determination of Fe(III) Adsorption

A total of 0.05 g of IIP was added to 50 mL of 5 ppm Fe(III) standard solution. The mixture was stirred using a magnetic stirrer for varying contact times of 30, 60, 90, 120, 150, and 180 minutes. The filtrate was analyzed using AAS to determine the Fe(III) adsorption capacity. The adsorption capacity (*Qe*) was calculated according to equation (2):

$$Qe = \frac{(Co - Ce) \times V}{m} \qquad (2)$$

Where Co (mg/L) is the initial Fe(III) concentration, Ce (mg/L) is the equilibrium concentration after adsorption, V (L) is the solution volume, and m (g) is the mass of the adsorbent.

Determination of Kinetic Models

Adsorption data were modeled into pseudo-first-order (PFO) (3) and pseudo-second-order (PSO) (4) Equations.

$$\log (q_e - q_t) = \log q_e - \frac{k_1}{2.303} t \qquad (3)$$

$$\frac{t}{q_t} = \frac{1}{k_{2qe^2}} + \frac{t}{q_e} \qquad (4)$$

Characterization of Fe(III)–IIP

The synthesized Fe–IIP polymers obtained via precipitation polymerization were characterized using several analytical techniques. FTIR was used to determine the types of functional groups, while AAS was used to determine the Fe(III) content in the samples. Furthermore, SEM was utilized to examine the surface morphology of the polymers.

RESULT AND DISCUSSION

Leaching of IIP

Table 1. Result of the IIP after the leaching process

Leaching (%)	Documentation IIP
98.866	

As shown in Table 1, HNO3 is highly efficient at leaching Fe(III) template ions from the polymer matrix, achieving a leaching (%) of 98.866%. This result indicates that almost all Fe(III) ions were effectively removed, confirming the strong oxidative properties of nitric acid in breaking the coordination bonds between Fe(III) ions and the functional monomers in the polymer structure.

The high leaching efficiency indicates the successful formation of specific recognition sites within the IIP. The resulting cavities have a suitable size, shape, and spatial arrangement, matching precisely with Fe(III) ions. Washing with aquadest ensured the complete removal of any remaining ions, as confirmed by AAS analysis of the filtrate. These findings correspond with Novianty *et al*. (2023), who noted that strong-acid treatment effectively removes template ions and supports the formation of stable, specific binding cavities in imprinted polymers.

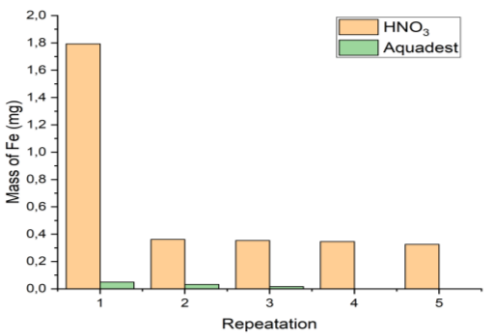

Figure 1. Comparison of Fe(III) ion release from IIP during repeated leaching with HNO_3 and Aquadest

Determination of Fe(III) Adsorption

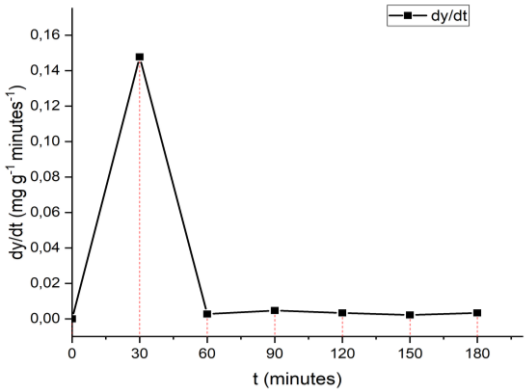

Figure 2. Effect of contact time on the adsorption rate (dy/dt) of Fe(III) ions onto Fe(III)-IIP

Table 2. Kinetic parameters of IIP adsorption

t (min)	Qe (mg g^{-1})
30	4.43
60	4.51
90	4.65
120	4.75
150	4.81
180	4.91

Based on Figure 2 and Table 2, contact time significantly affected the adsorption kinetics of Fe(III) ions onto the IIP. The adsorption rate (dy/dt) increased sharply during the initial stage, and the adsorption capacity (Qe) reached 4.43 mg g^{-1} at 30 minutes, which is characteristic of a rapid surface adsorption process driven by a high concentration gradient and the abundance of available active sites. As adsorption progressed, the gradual occupation of these sites reduced the driving force for mass transfer, causing a sharp decline in the adsorption rate at longer contact times (60–180 minutes). At this stage, the process became increasingly constrained by diffusion limitations and intraparticle mass-transfer resistance, limiting the transport of Fe(III) ions into the polymer network (Royani *et al*., 2024). Consequently, the adsorption system approached equilibrium, indicating that 30 minutes represents the kinetically optimum contact time before the dominance of a slow, diffusion-controlled adsorption regime, consistent with

adsorption kinetic theory and previously reported models.

Determination of Kinetic Models

Table 3. Kinetic parameters of IIP adsorption

Pseudo First Order (PFO)		Pseudo Second Order (PSO)	
Q_{max} (mg/g)	K_1 (min^{-1})	Q_{max} (mg/g)	K_2 (g/mg/min)
3.040	0.029	5.022	0.033

As shown in Table 3 and Figure 3, Fe(III) adsorption on IIP fits the PSO model (R^2 = 0.9993) better than the PFO model (R^2 = 0.8478). This high linearity suggests that the adsorption rate is controlled by the square of the number of unoccupied active sites, consistent with a chemisorption mechanism. The K_2 and the Qmax further confirm the strong affinity of the IIP toward Fe(III) ions. According to the PSO model, the adsorption of Fe(III) onto the IIP occurs through chemical interactions rather than physical forces. This suggests that specific imprinted sites play a key role in the binding process (Sangoremi, 2025). The high R^2 value and adsorption capacity confirm the selectivity and efficiency of the synthesized IIP.

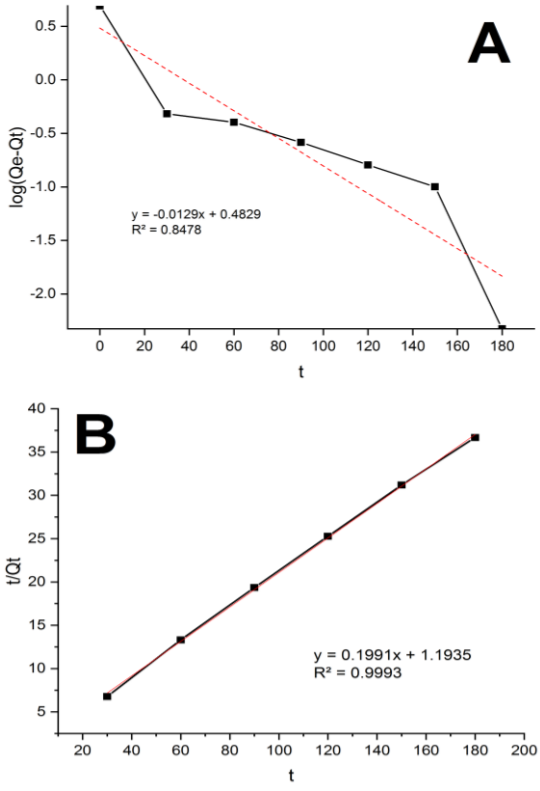

Figure 3. Kinetic models for Fe(III) adsorption onto IIP: (A) PFO model, (B) PSO model

Characterization FTIR

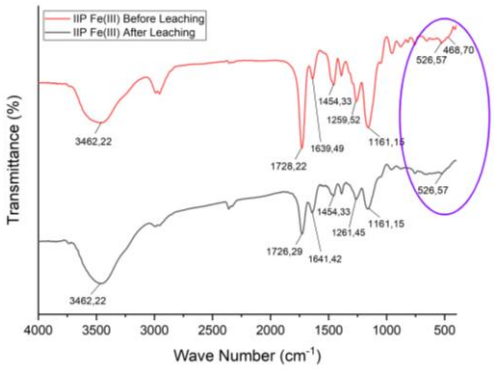

Figure 4. FTIR Spectra of IIP Fe(III) Before Leaching and IIP Fe(III) After Leaching

FTIR analysis was carried out at wavelengths between 400 and 4000 cm^{-1} for IIP Fe(III) before leaching and IIP Fe(III) after leaching samples (Figure 4). Before leaching, the spectrum showed a peak at 468.7 cm^{-1}, corresponding to Fe–O vibrations, indicating the presence of Fe(III) ions in the polymer matrix. This peak disappeared after leaching, confirming the removal of Fe(III) ions and the formation of selective recognition sites. Absorption bands at 1728.2 cm^{-1} (C=O), 1454.3 cm^{-1} (C=C), and 1161.1 cm^{-1} (C–O–C) verified the present of EGDMA. A weak band at 3462.2 cm^{-1} corresponded to –OH stretching from carboxylic groups, while the strong band at 1728.2 cm^{-1} again confirmed the presence of carbonyl groups from EDTA (Anggraini & Sianita, 2024).

Table 4. FTIR Characteristic Absorption Bands of Functional Groups

Functional Group	Wave number (cm^{-1})	
	Reference (Anggraini & Sianita, 2024) (Rahman *et al.*, 2017) (Nandiyanto *et al.*, 2023) (Permatasari & Sianita, 2025)	Result
Fe–O	468	468.70
–OH	3250-2650	3462.22
C=O	1728	1728.22
C=C	1453.7	1454.33
C–O–C	1156	1161.15

Characterization SEM

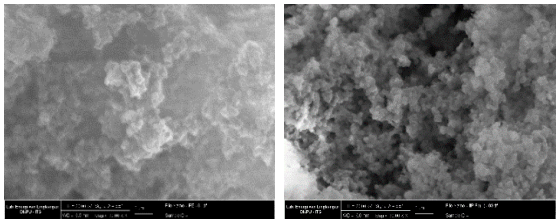

(a) (b)

Figure 5. SEM micrographs of (a) Blank Polymer (BP), (b) Ionic Imprinted Polymer (IIP) at a magnification of 20,000×.

SEM micrographs reveal distinct morphological differences between PB and IIP, reflecting differences in their polymerization mechanisms and chemical structures. The PB exhibits a smooth, compact, and non-porous surface, indicating the formation of a densely cross-linked polymer network in the absence of template ions, which results in a non-selective matrix lacking specific binding sites. In contrast, the IIP exhibits a rough, highly porous morphology with a relatively uniform particle distribution. This porous structure arises from coordination interactions between Fe(III) ions and functional ligands during the pre-polymerization stage, followed by the removal of the template ions. The leaching of Fe(III) generates imprinted cavities with specific size, shape, and chemical functionality that are complementary to Fe(III), serving as selective recognition sites (Lazar *et al*., 2023). These morphological and structural differences confirm successful synthesis of the ion-imprinted polymer and indicate that the IIP has an enhanced surface area, binding affinity, and chemical selectivity compared to the PB.

CONCLUSION

Fe(III)-IIP was successfully synthesized via precipitation polymerization using EDTA, MAA, EGDMA, and BPO as the main components. FTIR and SEM analyses confirmed successful imprinting and template removal, as evidenced by the disappearance of the Fe–O band and the formation of a porous IIP structure. The IIP had a highest *Qe* of 4.43 mg g^{-1} at 30 minutes. The kinetic study followed a PSO model (R^2 = 0.9993), indicating that chemisorption was the primary mechanism of the material's behavior. These results demonstrate that the IIP is a selective, stable, and suitable adsorbent for Fe(III)-contaminated water.

REFERENCES

Anggraini, H., & Sianita, M. M. (2024). The Effectiveness of Bulk Polymerization and Precipitation Polymerization on the Adsorption Capacity of Pb(II) Metal Ions Using Ionic Imprinted Polymer (IIP). *Indonesia Chimica Acta*, *17*(2). https://doi.org/http://dx.doi.org/10.70561/ica.v17i2.37146

Djunaidi, M. C., Fitriana, W., Lusiana, R. A., & Suseno, A. (2021). Adsorption of Fe (III) metal ion by ionic imprinted polymer (IIP) method with poly (ethylene glycol) diglycidyl ether (PEGDE) as a crosslinker. *Journal of Physics: Conference Series*, *1943*. https://doi.org/10.1088/1742-6596/1943/1/012168

Lazar, M. M., Ghiorghita, C. A., Dragan, E. S., Humelnicu, D., & Dinu, M. V. (2023). Ion-Imprinted Polymeric Materials for Selective Adsorption of Heavy Metal Ions from Aqueous Solution. *Molecules*, *28*(6), 2798. https://doi.org/10.3390/molecules28062798

Low, K. M., Lin, X., Wu, H., & Li, S. F. Y. (2024). Ion-Imprinted Polymer-Based Sensor for the Detection of Mercury Ions. *Polymers*, *16*(5), 1–13. https://doi.org/10.3390/polym16050652

Nandiyanto, A. B. D., Ragadhita, R., & Fiandini, M. (2023). Interpretation of Fourier Transform Infrared Spectra (FTIR): A Practical Approach in the Polymer / Plastic Thermal Decomposition. *Indonesian Journal of Science & Technology*, *8*(1), 113–126. https://doi.org/https://doi.org/10.17509/ijost.v8i1.53297

Ngatijo, Basuki, R., Nuryono, & Rusdiarso, B. (2019). Comparison of Au (III) Sorption on Amine-Modified Silica (AMS) and Quaternary Amine-Modified Silica (QAMS): A Thermodynamic and Kinetics Study. *Indonesian Journal of Chemistry*, *19*(2), 337–346. https://doi.org/10.22146/ijc.33758

Novianty, Edianta, J., Jorena, Saleh, K., Bama, A. A., Koriyanti, E., Ariani, M., & Royani, I. (2023). Synthesis of Fe(III)-IIPs (Ion Imprinted Polymers): Comparing Different Concentrations of HCl and HNO_3 Solutions in the Fe(III) Polymer Extraction Process for Obtaining the Largest Cavities in Fe(III)-IIPs. *Science and Technology Indonesia*, *8*(3), 361–366. https://doi.org/10.26554/sti.2023.8.3.361-366

Permatasari, Y., & Sianita, M. M. (2025). Optimization of pH Conditions for Lead Adsorption using Ion-Imprinted Polymer (IIP) with EDTA as Ligand. *Indonesian Journal of Chemical Analysis*, *08*(01), 31–39. https://doi.org/10.20885/ijca.vol8.iss1.art3

Putri, N. O., Ramadhanti, A. P., Widodo, L. U., & Pujiastuti, C. (2023). Pemisahan Ion Logam Perak Nitrat Dari Limbah Cair Pencucian Fotografi Melalui Metode Pertukaran Ion. *Jurnal Teknik Kimia*, *17*(2), 61–64. https://doi.org/https://doi.org/10.33005/jurnal_tekkim.v17i2.3783

Rahma, M., Hasri, & Pratiwi, D. E. (2023). Studi Adsorpsi Logam Fe (III) Menggunakan Komposit Kitin Silika Sekam Padi. *Jurnal Sainsmat*, *XII*(2), 200–210. http://ojs.unm.ac.id/index.php/sainsmat

Rahman, S. S. U., Qureshi, M. T., Sultana, K., Rehman, W., Khan, M. Y., Asif, M. H., Farooq, M., & Sultana, N. (2017). Single step growth of iron oxide nanoparticles and their use as glucose biosensor. *Results in Physics*, *7*, 4451–4456. https://doi.org/10.1016/j.rinp.2017.11.001

Royani, I., Edianta, J., Alfikro, I., Monado, F., Satya, O. C., & Virgo, F. (2024). Synthesis of Ion Imprinted Polymers (IIPs) Adsorbent Materials Using Fe (III) Leaching Process with Variation of Hydrochloric Acid Solvent Concentration and Heat Treatment. *Science and Technology Indonesia*, *9*(2), 336–344. https://doi.org/https://doi.org/10.26554/sti.2024.9.2.336-344

Sangoremi, A. A. (2025). Adsorption Kinetic Models and Their Applications: A Critical Review. *International Journal of Research and Scientific Innovation*, *XII*(V), 245–258. https://doi.org/10.51244/ijrsi.2025.120500019

Sappewali, Muke, C. M., Armus, R., & Aminah, S. (2024). Pengaruh Variasi Ketebalan Media Filtrasi Terhadap Penurunan Kadar Besi (Fe) Air Sumur Gali. *Jurnal Ilmu Alam Dan Lingkungan*, *15*(2), 33–42. https://journal.unhas.ac.id/index.php/jai2

Sufra, R., Panjaitan, J. R. ., Alhanif, M., Mustafa, Yusupandi, F., Adriansyah, E., Rahmadini, G., Raqin, M. R., Herawati, P., & Suzana, A. (2024). Intensifikasi Pengolahan Limbah Cair Laboratorium Melalui Proses Koagulasi dan Adsorpsi Studi Pengolahan Limbah Cair Laboratorium dengan Metode Kombinasi Fisika-Kimia. *Jurnal Talenta Sipil*, *7*(1), 266–275. https://doi.org/10.33087/talentasipil.v7i1.460

Veranica, Rahayu, A., & Maryudi. (2023). Review : Biomassa Sebagai Adsorbent untuk Pengolahan Logam Berat Pada Air Limbah Industri. *Prosiding Seminar Nasional Teknik Kimia "Kejuangan,"* 1–6.

Zhang, H., Rush, Z., Penn, Z., Dunn, K., Asmus, S., Cooke, C., Cord, Z., Coulter, S., & Morris, C. (2024). Films Floating on Water Surface: Coupled Redox Cycling of Iron Species (Fe(III)/Fe(II)) at Soil/Water and Water/Air Interfaces. *Water*, *16*(9), 1298. https://doi.org/10.3390/w16091298